

Constrained auxiliary particle filtering for bearings-only maneuvering target tracking

ZHANG Hongwei* and XIE Weixin

Automatic Target Recognition Key Laboratory, Shenzhen University, Shenzhen 518060, China

Abstract: To track the nonlinear, non-Gaussian bearings-only maneuvering target accurately online, the constrained auxiliary particle filtering (CAPF) algorithm is presented. To restrict the samples into the feasible area, the soft measurement constraints are implemented into the update routine via the ℓ_1 regularization. Meanwhile, to enhance the sampling diversity and efficiency, the target kinetic features and the latest observations are involved into the evolution. To take advantage of the past and the current measurement information simultaneously, the sub-optimal importance distribution is constructed as a Gaussian mixture consisting of the original and modified priors with the fuzzy weighted factors. As a result, the corresponding weights are more evenly distributed, and the posterior distribution of interest is approximated well with a heavier tail. Simulation results demonstrate the validity and superiority of the CAPF algorithm in terms of efficiency and robustness.

Keywords: bearings-only maneuvering target tracking, soft measurement constraints, constrained auxiliary particle filtering (CAPF).

DOI: 10.21629/JSEE.2019.04.06

1. Introduction

Bearings-only tracking (BOT) refers to estimating the current object states (such as position and velocity) by using only the noise-corrupted bearings measured by a single moving passive sensor or multiple static passive sensors [1–4]. In the Bayesian context, the process is modeled as the state estimation of a dynamic Markov process, where the probability density function (PDF) of the current state is required when given the available measurement, i.e., the posterior PDF, which consists of two stages that are performed at every step: prediction and update process. In the update phase, the Bayes' rule is applied to the prior PDF via the measurement function yielding the posterior PDF. In the linear Gaussian models or cases where the nonlinear

effects are mild, the posterior PDF can be calculated analytically by the Kalman filter (KF), which is expected to provide accurate enough representation of the true posterior with a low computational load. For BOT, besides the measurement noise, maneuvering target tracking faces two main interrelated challenges: the inherently nonlinearity and the target motion uncertainty. Therefore, it is hard to establish a finite-dimensional optimal Bayesian filtering method with a closed-form solution, and approximations are required in practice.

For the state nonlinear filtering (NFL), the Taylor series expansions (TSE) is the fundamental method [5], and the well-known first order one, extended KF (EKF), may often yield good estimates and accurate covariance estimates. However, when implemented in a Cartesian state space, it can diverge in many instances, yielding poor estimates with optimistic covariance matrix [1]. Uncensored KF (UKF) is the alternate typical KF-type method [6,7]. It can provide more flexible and accurate estimate than that of the EKF via sampling some Sigma-points to propagate and match the higher order moment of the state posterior distribution. Nevertheless, the KF-based filters have the drawback that the conditional densities, both the state and measurement noises, are assumed as Gaussian [5]. For the nonlinear, non-Gaussian cases, the particle filter (PF) is the alleviated approach [8,9]. The method approximates the posterior distribution by a complete representation in an online manner via drawing a finite number of samples. The traditional EKF and UKF can be used to generate the proposed distribution, and they are known as PF-EKF and PF-UKF [10]. The estimate performance of the EKF, UKF, PF-EKF, PF-UKF, and PF is compared and analyzed in [11]. Note that the standard sequence importance resample (SIR) filter is vulnerable to the particle impoverishment, and the auxiliary particle filter (APF) [12,13] is an alternative algorithm which solves essentially this problem. Through exchanging the order of the sampling and resampling steps, a greater number of distinct samples can

Manuscript received November 19, 2018.

*Corresponding author.

This work was supported by the National Natural Science Foundation of China (61773267) and the Shenzhen Fundamental Research Project (JCYJ20170302145519524; 20170818102503604).

be propagated with higher probability masses, following a closer approximation to the true posterior PDF.

On the other hand, multiple-model (MM) approaches have been generally regarded as the mainstream method for the maneuvering target tracking with motion model uncertainties [2,14]. The interacting MM (IMM)-based estimators [15,16] are common estimation techniques, and the motion models can switch between each other in a Markov probabilistic manner. Generally, the method adopts the EKF or UKF for the state NFL, and the quality and complexity of model design should be traded off.

It has been illustrated in [17,18] that, in practice, the approximation of the posterior distribution is accurate only in the feasible region of interest. Therefore, two important points should be considered. First, the constraints condition can be incorporated into the dynamic estimate procedure [19,20]. Second, the posterior should be approximated as a Gaussian mixture in the different sub-area [2]. Angel et al. [21] proposed the mixture truncated UKF that can improve the filtering performance especially when the current measurement is sufficiently precise, and it requires that the measurement equation should be continuous and bijective rigorously. It should be noted that considering the bounds into the updating procedure means that the conditional state density becomes non-Gaussian, and then the conventional Kalman-type filters are not suitable. For this problem, the constrained particle filtering methods arose [22,23], and the convergence of the constrained particle filter algorithm was proved in the mathematical viewpoint [24,25].

In the particle filtering context, constructing a suitable importance proposal distribution is the critical step to reduce the drawn samples size and enhance the estimate accuracy [26,27], the modified sub-optimal importance distribution should produce adaptability. In [28], an auxiliary PF with inequality constraints was proposed, the drawn particles were restricted to the feasible area via the numerical optimal method, resulting in more accurate tracking performance. Nevertheless, the algebraic inequality was specially set and must be strictly satisfied. Still, imposing the constraint condition as the potential prior knowledge into the bearings-only maneuvering target tracking is generally challenging and has attracted considerable attention [29]. Therefore, an auxiliary truncated particle filtering (ATPF) was presented in [30], through modifying the priori PDF, and the algorithm handled the stochastic maneuvering motion successfully, especially for the sparse sampling cases. Nevertheless, for the uniform sampling scenario, the overall filtering performance after the maneuvering motion is not smooth due to the potential narrow importance proposal distribution. Based on the Rao-Blackwell theorem that computing the conditionally Gaus-

sian component can generally improve the accuracy compared with any finite set and reduce the variance error for the pure Monte Carlo method [31,32]. A constrained multiple modal particle filtering was presented in our recent work [33], the motion model was marginalized out, and the nonlinear filtering was dealt with effectively by making use of the sequential Monte Carlo (SMC) method. The algorithm is effective for both the uniform and sparse sampling environment. Considering that, the computation load is high due to the discrete particle calculation, and like the IMM-based estimators, the model refinement is a challenging problem.

Instead, the constrained auxiliary particle filter (CAPF) algorithm proposed in this paper departs from the aforementioned methods and aims to track the bearings-only maneuvering target accurately online. The proposed algorithm focuses on the update process, and the soft measurement constraints are implemented by a heuristic optimizer [34,35]. First, to approximate the posterior distribution well, the importance proposal function should be constructed with a heavier distribution. To do this, the center of the resample stage is approximated as a ℓ_1 regularization problem based on the minimized mean square error (MMSE) criterion.

Meanwhile, to improve the sample diversity and likelihood, the soft measurement constraints are involved into the update stage along with the motion kinetics auxiliary variables as the latest measurement arrives every time step. Second, to enhance the robustness, the modified sub-optimal importance distribution is established as a Gaussian mixture consisting of the original and the modified prior PDF, allowing the adaption of the up-to-date measurement and the feedback from the past measurement simultaneously. And the effect is weighted by a self-adapt fuzzy factor, respectively. Hence, the accuracy can be improved by the significant samples which can characterize the true posterior PDF well. Meanwhile, the computation complexity can be traded off due to the omission of the resampling operation in the second stage in the particle filtering context.

The remainder of the sections of the paper is organized as follows. The stratification of the proposed CAPF is described in Section 2. Monte Carlo simulations for bearings-only maneuvering target tracking to demonstrate the validity and superiority of the proposed algorithm is given in Section 3. Finally, Section 4 concludes, pointing out the features and future work of the proposed CAPF algorithm.

2. Stratification of the CAPF algorithm

The stratification of the proposed CAPF algorithm will be explained in this section. The stochastic model system is introduced in Section 2.1. The motivation and problem statement are described in Section 2.2. The design and dis-

cussion are described in Section 2.3. Summary and convergence analysis are given in Section 2.4.

2.1 Dynamic system modeling

Consider the discrete-time nonlinear model system as a dynamic Markov process

$$\mathbf{X}_{k+1} = \mathbf{F}_k(\mathbf{X}_k) + \mathbf{V}_k \quad (1)$$

$$\mathbf{Z}_k = \mathbf{H}_k(\mathbf{X}_k) + \mathbf{e}_k \quad (2)$$

where k is the discrete time index, \mathbf{X}_k and \mathbf{Z}_k denote the discrete state vector and the measurement sequence. \mathbf{F}_k and \mathbf{H}_k are the state transition and the measurement matrix, and $\mathbf{V}_k \sim N(0, \sigma_k)$ and $\mathbf{e}_k \sim N(0, R_k)$ denote the process and measurement noises, respectively, where $N(\mathbf{m}, \mathbf{p})$ denote the normal distribution with the mean \mathbf{m} and the covariance \mathbf{p} .

The bearings measurements are provided by two stationary passive sensors. The measurement function in (2) is

$$\begin{pmatrix} \theta_{j,k} \\ \beta_{j,k} \end{pmatrix} = \mathbf{H}(\mathbf{X}_k) = \begin{pmatrix} \arctan\left(\frac{Y_{j,k-1} - Y_{s_j}}{X_{j,k-1} - X_{s_j}}\right) \\ \arctan\left(\frac{Z_{j,k-1} - Z_{s_j}}{\sqrt{(X_{j,k-1} - X_{s_j})^2 + (Y_{j,k-1} - Y_{s_j})^2}}\right) \end{pmatrix}, \quad j = 1, 2 \quad (3)$$

where $j = 1, 2$ denotes the j th passive sensor which supplies the measurements at time k . $\theta_{j,k}$ and $\beta_{j,k}$ denote the azimuth and the elevation angle of the aircraft measured by the i th sensor at time k , respectively, which are transmitted to the fusion node with zero time delay. $\mathbf{X}_{j,k} = (X_{j,k}, \dot{X}_{j,k}, Y_{j,k}, \dot{Y}_{j,k}, Z_{j,k}, \dot{Z}_{j,k})^T$ defines the target location in the 3D space from the j th sensor at time k , where $(X_{j,k}, Y_{j,k}, Z_{j,k})$ and $(\dot{X}_{j,k}, \dot{Y}_{j,k}, \dot{Z}_{j,k})$ represent the target location and velocity vector, respectively. $X_{s_j} = (X_{s_j}, Y_{s_j}, Z_{s_j})$ denotes the location of the j th sensor; $\mathbf{R}_{s_j} = \begin{bmatrix} 1 & 0 \\ 0 & 1 \end{bmatrix} \sigma_e^2$ denotes the measurement noise of the j th sensor. The measurement noises in each sensor are independent of each other and the process noise.

2.2 Problem statement

In the Bayesian inference frame, to approximate the discrete-time nonlinear filtering (NLF), all the methods amount to approximating the two major steps, predication and the update process. Generally, for any form of the

prior, the KF update can always be employed [21]. However, the KF-type approximations cannot work properly for the following two cases.

Case 1 If the likelihood is multimodal, the associated posterior is multimodal correspondingly.

Case 2 Even if the likelihood is unimodal, the current measurement is precise compared with the prior. In this regard, the posterior PDF of the interest should be approximated as a mixture term as

$$p(\mathbf{X}_k | \mathbf{Z}_k) \propto \sum_{i=1}^m p_{lik,i}(\mathbf{Z}_k | \mathbf{X}_k) p_i(\mathbf{X}_k | \mathbf{X}_{k-1}) \alpha_k^i, \quad \sum_{i=1}^m \alpha_k^i = 1 \quad (4)$$

where m is the size of total components, $p_{lik,i}(\cdot)$ and $p_i(\cdot)$ are the i th likelihood and the prior PDF, respectively. α_k^i is the associated weight. For easy explanation, the time index and the condition on the past measurements are omitted.

As illustrated in [22], in practice, the approximation of the posterior distribution is accurate only in the feasible region of interest, and it can be implemented by using the soft measurement constraints in view of the fact that the measurement noise is generally bounded supported. Thus, it can be reasonable to define the first assumption AP1), that the density of the additive measurement noise in (2), $p_{e_k}(\mathbf{e}_k)$, has a connected but bounded support, i.e.,

$$p_{e_k}(\mathbf{e}_k) = 0, \quad \mathbf{e}_k \notin \wp_k \subset \mathbb{R}^{d_z} \quad (5)$$

where \mathbb{R}^{d_z} is the d_z dimensional connected measurement area. \wp is the feasible area of interest that can be defined as

$$\wp_k = \{\mathbf{X}_k = [(\mathbf{H}^{-1}(\mathbf{Z}_k - \mathbf{e}_k))^T, \mathbf{b}^T]^T\} \quad (6)$$

where $\mathbf{H}^{-1}(\cdot)$ is the inverse function of the measurement function, and it should meet the second assumption AP2), that the measurement function $\mathbf{H}(\cdot)$ is bijective and continuous. Due to the inherent high nonlinearity of the measurement function for the BOT, the NFL can be approximated instead of the third assumption AP3), that the nonlinear observation function $\mathbf{H}(\cdot)$ can be linearized locally.

Furthermore, for the BOT application in this paper, to deal with the common sample degeneracy phenomenon, we incorporate the target kinetics features as the auxiliary variables into the update process. Let $r_{1:k}$ denote the auxiliary variables set, which is irrelevant to the observation sequence z_k . Thus, the modified posterior PDF with constraints can be acquired by the Bayes' rule, that is

$$p(\mathbf{X}_{0:k} | \mathbf{Z}_{1:k}, r_{1:k}) = \frac{p(\mathbf{Z}_k | \mathbf{X}_{0:k}, r_{1:k}) p(\mathbf{X}_k | \mathbf{X}_{1:k-1}, \mathbf{Z}_{1:k-1}, r_{1:k}) p(\mathbf{X}_{1:k-1} | \mathbf{Z}_{1:k-1}, r_{1:k-1})}{p(\mathbf{Z}_k, r_k | \mathbf{Z}_{1:k-1}, r_{1:k-1})} =$$

$$\frac{p_{\varphi}(\mathbf{Z}_k - h(a_k))\chi(\mathbf{Z}_k|\mathbf{X}_k, r_k)p(\mathbf{X}_k|\mathbf{X}_{1:k-1}, \mathbf{Z}_{1:k-1}, r_{1:k})p(\mathbf{X}_{1:k-1}|\mathbf{Z}_{1:k-1}, r_{1:k-1})}{p(\mathbf{Z}_k, r_k|\mathbf{Z}_{1:k-1}, r_{1:k-1})} \propto \frac{p_g(\mathbf{Z}_k|\mathbf{X}_k, r_k)p_1(\mathbf{X}_k|\mathbf{X}_{k-1}, \mathbf{Z}_{k-1}, r_{1:k})p(\mathbf{X}_{1:k-1}|\mathbf{Z}_{1:k-1}, r_{1:k-1})}{\varepsilon_k} \quad (7)$$

s.t. $\{\mathbf{X}_k, \mathbf{Z}_k\} \in \wp_k$

where ε_k is a normalizing constant [11,14], and $h(\cdot)$ denotes the nonlinear function of a_k . $\chi(\cdot)$ is the indicator function on the constrained sub-area that can be defined as

$$\chi_{\wp_k}(\mathbf{X}_k) = \begin{cases} 0, & e_k \notin \wp_k \subset \mathbb{R}^{d_z} \\ 1, & e_k \in \wp_k \subset \mathbb{R}^{d_z} \end{cases} \quad (8)$$

Compared with (4), it can be known from (7) that, besides the current measurement and kinematics auxiliary variables, the constraints condition is incorporated into the estimate proceeding.

Now the problem (4) can be converted to approximate the components of priors. To derive the Gaussian approximation for the prior PDF, the target state vector can be presented as $\mathbf{X}_k = [\mathbf{a}_k^T, \mathbf{b}_k^T]^T$. $\mathbf{a}_k \in \mathbb{R}^{d_a}$ and $\mathbf{b}_k \in \mathbb{R}^{d_b}$ denote the d_a dimension position and d_b dimension velocity vectors, respectively, and $d_{\mathbf{X}} = d_a + d_b$. Thus, the mean matrix $\widehat{\mathbf{X}}_{p_{i,k}}$ and the covariance matrix $\mathbf{P}_{i,k}(\cdot)$ of the prior PDF $p_{i,k}(\cdot)$ can be factorized as

$$\widehat{\mathbf{X}}_{p_{i,k}} = \begin{bmatrix} \mathbb{E}[\mathbf{a}_{i,k}] \\ \mathbb{E}[\mathbf{b}_{i,k}] \end{bmatrix} = \begin{bmatrix} \boldsymbol{\mu}_{\mathbf{a}_{i,k}} \\ \boldsymbol{\mu}_{\mathbf{b}_{i,k}} \end{bmatrix} \quad (9)$$

$$\widehat{\mathbf{P}}_{i,k} = \begin{bmatrix} \text{Cov}[\mathbf{a}_{i,k}] & \text{Cov}[\mathbf{a}_{i,k}, \mathbf{b}_{i,k}] \\ \text{Cov}[\mathbf{b}_{i,k}, \mathbf{a}_{i,k}] & \text{Cov}[\mathbf{b}_{i,k}] \end{bmatrix} = \begin{bmatrix} \sum_{\mathbf{a}_{i,k}} & \sum_{\mathbf{a}_{i,k}, \mathbf{b}_{i,k}} \\ \left(\sum_{\mathbf{a}_{i,k}, \mathbf{b}_{i,k}} \right)^T & \sum_{\mathbf{b}_{i,k}} \end{bmatrix} \quad (10)$$

where $i = 0, 1$ denotes the original and the modified ones.

The mean and the covariance can be calculated by

$$\mu_{\mathbf{a}_{i,k}} = \int a p_i(a; \mathbf{Z}_k) da = \widehat{a}(\mathbf{Z}_k), \quad i = 0, 1 \quad (11)$$

$$\Sigma_{\mathbf{a}_{i,k}} = \int (\mathbf{a}_{i,k} - \boldsymbol{\mu}_{i,a})(\mathbf{a}_{i,k} - \boldsymbol{\mu}_{i,a})^T \mathbf{P}_i(a; \mathbf{Z}) da = \widetilde{\mathbf{H}}^{-1} \mathbf{R} (\widetilde{\mathbf{H}}^{-1})^T, \quad i = 0, 1 \quad (12)$$

where \mathbf{H}^{-1} is the Jacobia of the measurement function at \mathbf{a}_k . The estimate of $\mu_{\mathbf{a}_{0,k}}$ and $\sum_{\mathbf{a}_{0,k}}$ can be found in [22].

Taking into account the measurement, algebraic constraints always imply that the marginal densities of the state in a nonlinear system are generally non-Gaussian, even when the measurement noise and the state noise inputs are the Gaussian model. In this regard, we propose

the CAPF to deal with bearings-only maneuvering target tracking, and the implementation will be given in Section 2.3.

2.3 Design of the CAPF algorithm

2.3.1 Brief extension of APF algorithm

In the filtering context, our objective is to calculate a numerical solution of the posterior PDF $p(\mathbf{X}_{1:k}|\mathbf{Z}_{1:k})$ ($k \geq 1$) sequentially in time. SMC works by producing a Monte Carlo approximation to the posterior PDF which can be easily updated to incorporate the current measurement while it arrives. In [8], it has been demonstrated that, in the sense to minimize the variance of the importance weights, the optimal importance distribution has the form as

$$p(\mathbf{X}_k|\mathbf{X}_{1:k-1}) = \frac{p(\mathbf{Z}_k|\mathbf{X}_k)p(\mathbf{X}_k|\mathbf{X}_{k-1})}{p(\mathbf{Z}_k|\mathbf{X}_{k-1})} \quad (13)$$

where the components as the likelihood and prior PDF are defined in (4).

The standard SIR filter is not robust to the sample impoverishment, and the estimate accuracy may be reduced due to the additional random noise introduced by the resampling approach. The APF [12] is an alternative method which solves essentially this problem through exchanging the order of the sampling and resampling step.

In a sense, the APF is a look-ahead algorithm in which we can use the information from the next observation at the time $k+1$ to determine which particles will survive in areas of high probability masses at the given time k . In this regard, the center of the resampling step in the first stage should be predicted to reflect the effective information sufficiently.

According to (7), considering the soft measurement constraints, the associated modified prior PDF $p_1(\cdot)$ becomes a truncated version of the prior PDF $p_0(\cdot)$, that is

$$p_1(\mathbf{X}_k|\mathbf{X}_{k-1}, \mathbf{Z}_k) \propto \frac{\chi(\mathbf{Z}_k|\mathbf{X}_k, r_k)p_0(\mathbf{X}_k|\mathbf{X}_{1:k-1}, \mathbf{Z}_{1:k-1}, r_{1:k})}{\varepsilon_k} \quad (14)$$

In view of (14), besides the latest measurement \mathbf{Z}_k and auxiliary variables $r_{1:k}$, the measurement constraints of interest are adopted to define the modified truncated prior PDF.

2.3.2 Approximating the center of the resampling stage as ℓ_1 regularization problem

Once a non-Gaussian posterior PDF is approximated by a Gaussian one, the optimal inference disappears. We use the truncated Newton method on the interior point method (IPM) optimization method [34] to approximate it. The method demands that the state initial point should be into the feasible area. The position with maximum likelihood is selected, and the adaptive locating method can be found in our recent work [33].

To enhance the accuracy, especially for the arbitrary changes in motion models, the motion kinetics features are introduced as the auxiliary variables in (15), and the modified maximum likelihood position can be computed as follows:

$$\hat{\varphi}(\mathbf{Z}_k) = \mu_{a,0} + K_k(\tilde{a}(\mathbf{Z}_k) - \tilde{\mathbf{H}}_k^{-1}(\mu_{a,0})) \quad (15)$$

$$K_k = \frac{(T^2 \cdot \mathbf{V}_k^2 \cdot (\sigma_{V_k})^2)}{(\lambda(\sigma_{m_k})^2 + T^2 \cdot \mathbf{V}_k^2 \cdot (\sigma_{V_k})^2)} \quad (16)$$

where \mathbf{V}_k denotes the current estimated velocity, T is the interval time, λ is a constant, σ_{m_k} and σ_{V_k} denote the measurement noise and innovation covariance, respectively. $\tilde{\mathbf{H}}_k^{-1}$ denotes the Jacobian operation evaluated at $\mu_{a,0,k}$.

Mathematically, according to the criterion of MMSE, in view of (1), the objective function can be constructed as

$$\begin{aligned} \hat{\mathbf{X}}_k^c &= \arg \min_{\mathbf{X}_k} \left(\sum_{l=1}^k [\mathbf{X}_{k+1} - f_k(\mathbf{X}_k)]^2 \right) \\ \text{s.t. } \{\mathbf{X}_k^i\}_{i=1}^{N_s} &\in \mathcal{G}_k \end{aligned} \quad (17)$$

where the subscript index i denotes the i th step, and the superscript index k is the arriving time.

The soft constraints can be implemented by adding a regularization term [19]. The log-norm form of the ℓ_1 -regularization of the target vector to estimate can be selected as the barrier function, i.e.,

$$B(\mathbf{X}_k) = - \sum_{k=1}^K \ln[\ell_1(\mathbf{X}_k)] \quad (18)$$

and the estimate accuracy and convergence rate can be well traded off.

By subsisting (18) into (17), to solve (17) can be converted to solving (19) without constraints. With a suitably chosen parameter ρ_k , the corresponding augmented objective function is formed as

$$\bar{\mathbf{X}}_k^c = \arg \min_{\mathbf{X}_k} \sum_{l=1}^k \{ [\mathbf{X}_{k+1} - f_k(\mathbf{X}_k)]^2 - \rho_k \ln[\ell_1(\mathbf{X}_k)] \} \quad (19)$$

where the parameter ρ_k is a descending sequence, and the initial value equals 1.

The computation complexity is roughly proportional to amount of the vector variables to estimate, and by using the golden section into the backtracking line research, the global optimal solution is

$$\hat{\mathbf{X}}_k^l = \mathbf{X}_0 - s \cdot d_k^l \quad (20)$$

where s is the step size, which can always be selected as 1. d_k is the search direction which can be defined as

$$d_k = (\nabla^2 f_k)^{-1} (\nabla f_k) \big|_{\mathbf{X}=\mathbf{X}_0} \quad (21)$$

where f_k is the corresponding augmented objective function.

Since the optimal solution acquired by the derivation above is regarded as the center of the feasible area, then the moment can be seen as the covariance of the modified Gaussian distribution, i.e.,

$$\mathbf{P}_k^c = E((\hat{\mathbf{X}}_k^i - \bar{\mathbf{X}}_k^c)(\hat{\mathbf{X}}_k^i - \bar{\mathbf{X}}_k^c)^T). \quad (22)$$

Ultimately, the modified prior PDF can be approximated as the Gaussian form

$$p_1 \approx N(\mathbf{X}_k^i, \bar{\mathbf{X}}_k^c, \mathbf{P}_k^c). \quad (23)$$

The key idea of the CAPF is that, at every instance, the samples selected to propagate into the next step should be those which have a higher likelihood. Doing this can adapt and enhance the statistic efficiency of the sampling procedure and reduce the error of the covariance significantly.

2.3.3 Constructing the mixture importance distribution

Constructing the importance distribution with a higher conditional likelihood is an essential strategy to diagnose the sample impoverishment and improve the statistical efficiency of the sampling procedure. In particular, it often helps to smooth the outliers by considering the past measurements, allowing the feedback and adaption.

In view of (4) and (13), by substituting the mixture priors, the modified suboptimal importance distribution can be constructed as

$$\pi(\cdot) \propto \frac{[\alpha_k p_{1,k} + (1 - \alpha_k) p_{0,k|k}]}{\varepsilon_k} \quad (24)$$

where $\alpha_k \in [0, 1]$ is the scaling factor to control the weight of the informative measurement from the original and the modified prior PDFs.

In view of (3) and (23), it can be defined by the fuzzy logic Gaussian function (25) and (26) effectively,

$$g(\hat{\mathbf{X}}_{i,k}) = \frac{1}{\sqrt{|\mathbf{P}_{i,k}|}}.$$

$$\exp \left(-\frac{1}{2} (\mathbf{Z}_{i,k} - \mathbf{H}(\hat{\mathbf{X}}_{i,k}))^T (\mathbf{S}_{i,k})^{-1} (\mathbf{Z}_{i,k} - \mathbf{H}(\hat{\mathbf{X}}_{i,k})) \right),$$

$$i = 0, 1 \quad (25)$$

$$\alpha_k = \frac{g(\widehat{\mathbf{X}}_{i,k})}{(g(\widehat{\mathbf{X}}_{0,k}) + g(\widehat{\mathbf{X}}_{1,k}))} \quad (26)$$

where $S_{i,k}$ is the covariance innovation of the i th measurement at time k , and the parameter α_k should tend to 1 when the current measurements are very informative.

In experience, the improved version of APF only including one resampling step each time outperforms the original two stage resampling method [8,12]. During the sampling procedure, it can enhance the statistical efficiency and reduce the error covariance substantially through sampling the samples with a higher conditional likelihood rather than duplicating many times from samples with a very low likelihood.

2.3.4 State estimate

Like the generic PF, after the sampling step, a Monte Carlo approximation of the importance proposal distribution for the CAPF algorithm is acquired by the associated unnormalized importance weights that are given by

$$\begin{aligned} \omega_k^i &\propto \frac{p(\mathbf{X}_{0:k}^i | \mathbf{Z}_{1:k}, r_{1:k})}{\pi(\mathbf{X}_{0:k}^i | \mathbf{Z}_{1:k}, r_{1:k})} \propto \\ &\omega_k^i \frac{p(\mathbf{Z}_k | \mathbf{X}_k^i, r_{1:k}) p_1(\mathbf{X}_k^i | \mathbf{Z}_k, \mathbf{X}_{k-1}^i, r_{1:k})}{\pi(\mathbf{X}_k^i | \mathbf{X}_{0:k-1}^i, \mathbf{Z}_k, r_{1:k})} \propto \\ &\omega_{k-1}^i p(\mathbf{Z}_k | \mathbf{X}_k^i, r_{1:k}) \end{aligned} \quad (27)$$

which can be normalized as

$$\tilde{\omega}_k^i = \omega_k^i \left[\sum_{i=1}^{N_s} \omega_k^i \right]^{-1}. \quad (28)$$

Finally, the mean and the covariance of the target state are estimated by

$$\widehat{\mathbf{X}}_k = \sum_{i=1}^{N_s} \tilde{\omega}_k^i \mathbf{X}_k^i, \quad (29)$$

$$\mathbf{P}_k = \sum_{i=1}^{N_s} \tilde{\omega}_k^i (\widehat{\mathbf{X}}_k^i - \widehat{\mathbf{X}}_k) (\widehat{\mathbf{X}}_k^i - \widehat{\mathbf{X}}_k)^T \quad (30)$$

where N_s is the sample size.

2.3.5 Summary and convergence analysis

To summarize, one straightforward cycle of the CAPF algorithm proceeds as follows.

Step 1 Initialization. Set state PDF, $\mathbf{X} \sim N(\overline{\mathbf{X}}_0, p_0)$. Sample $\mathbf{X}_1^i \sim \pi(\mathbf{X}_1 | \mathbf{Z}_1)$ at the time $k = 1$ and update the trajectories.

Step 2 Approximate the first two moments of the center of the feasible region by using the backtracking line search.

Step 3 Construct the modified mixture proposal distribution (24) with the dual feasible points.

Step 4 Resample particles according to the corresponding weight (27).

Step 5 Estimate the state mean $\widehat{\mathbf{X}}_k^c$ and the covariance \mathbf{p}_k by using (29). Update time k .

The simple reinterpretation of the CAPF shows us several things:

(i) The importance distribution should be constructed with thicker tails. Then, a greater number of distinct samples can be propagated to approximate the posterior PDF.

(ii) The predictive likelihood should be approximated to be compatible with the motion model in the sense that it can encode at least the same degree of uncertainty as the true model. Introducing the motion kinetics features can adapt, and the mixture form can help avoid the outliers.

(iii) The numerical method uses the usual MMSE criterion to ensure that the error variance induced in the update procedure remains finite.

Nevertheless, the importance weight function derived above will often be not upper bounded on the area in (1), or it could produce divergence due to a very large or even infinite variance. The problem can be avoided by the simple elaboration given below.

With the convergence analysis in [24], under the nonlinear Bayesian filtering framework, in the feasible area \mathfrak{R} , if the importance weight is upper bounded for any state, then for all function $f_t \in \mathfrak{R}$, there exists the upper bound which is independent of N , i.e.,

$$\begin{aligned} \mathbb{E} \left[\left(\frac{1}{N} \sum_{i=1}^N f_t(\mathbf{X}_{0:t}^i) - \int f_t(\mathbf{X}_{0:t}) p(d\mathbf{X}_{0:t} | \mathbf{Z}_{1:t}) \right) \right] &\leq \\ c_t \frac{\|f_t\|}{N} \end{aligned} \quad (31)$$

where the subscript t denotes the series time, and c_t is a constant independent from the time step.

For the proposed CAPF algorithm, the constrained state upper boundary can be guaranteed by the index function (8) imposed onto the area of interest as follows:

$$|(f_{k+1}(\mathbf{X}) - f_k(\mathbf{X})), \gamma| \leq c_k \delta \|\gamma\| \quad (32)$$

where φ is the auxiliary variable which has a finite normal $\delta \|\varphi\|$.

Thus, the covariance error has the upper boundary which can be presented as

$$\lim_{N \rightarrow \infty} \sup |(\widehat{v}_{k+1}^N - v_k), r| \leq \xi c_k \|\gamma\| \quad (33)$$

where ξ is the finite constant coefficient.

Thus the proposed CAPF algorithm with soft measurement constraints can converge theoretically.

3. Simulation study

To study the filtering performance of the CAPF for the BOT problem, a set of 100 Monte Carlo runs are carried out based on the two simulation scenarios: a periodic sampling simulation scenario in Section 3.1, and an aperiodic and sparse sampling scenario in Section 3.2. The setting parameters and the target motion models for the IMM-based filters can be referenced as our recent work [33]. For the algorithms compared in this paper, the transition matrix is selected as the first constant velocity model, i.e.,

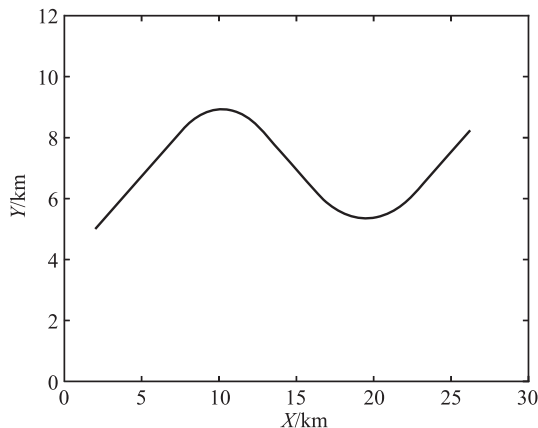
$$\mathbf{X}_k = \begin{bmatrix} 1 & T & 0 & 0 & 0 & 0 \\ 0 & 1 & 0 & 0 & 0 & 0 \\ 0 & 0 & 1 & T & 0 & 0 \\ 0 & 0 & 0 & 1 & 0 & 0 \\ 0 & 0 & 0 & 0 & 1 & T \\ 0 & 0 & 0 & 0 & 0 & 1 \end{bmatrix} \mathbf{X}_{k-1} + \begin{bmatrix} T^2/2 & 0 & 0 \\ T & 0 & 0 \\ 0 & T^2/2 & 0 \\ 0 & T & 0 \\ 0 & 0 & T^2/2 \\ 0 & 0 & T \end{bmatrix} \mathbf{V}_k \quad (34)$$

where T denotes the sampling interval, and \mathbf{V}_k is the process noise which is a Gaussian form with a 3×3 independent identical distribution (i.i.d.) matrix.

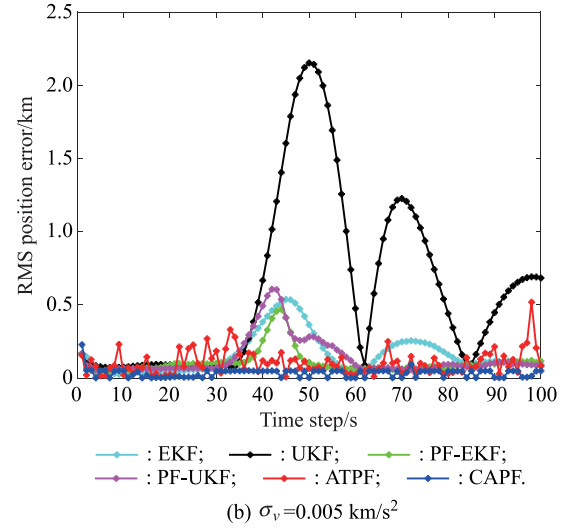
For the Monte Carlo runs, we reference two performance parameter matrices that are defined in [33]: (i) root mean square error (RMSE); (ii) root time-averaged mean square error (RTAMSE).

3.1 Periodic sampling case

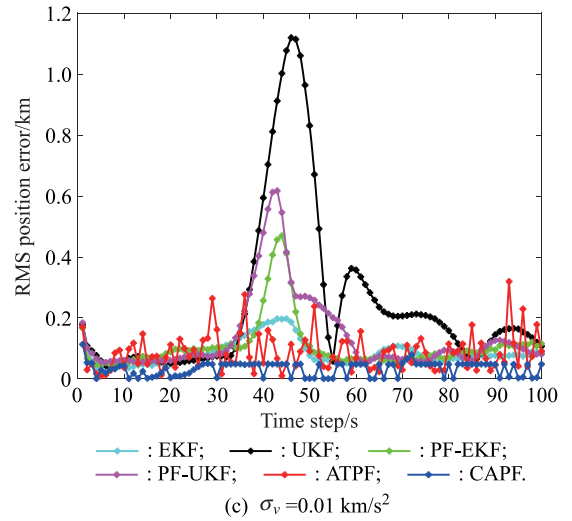
For the periodic sampling scenario designed in this subsection, we will study the filtering performance among the conventional EKF, UKF, PF-EKF and PF-UKF [6,11], the ATPF in [30] and the proposed CAPF. Fig. 1(a) shows the simulated trajectory.



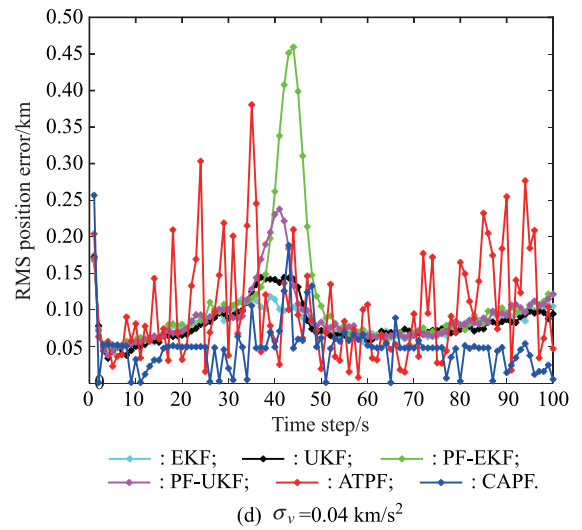
(a) Simulated true trajectory



(b) $\sigma_v = 0.005 \text{ km/s}^2$



(c) $\sigma_v = 0.01 \text{ km/s}^2$



(d) $\sigma_v = 0.04 \text{ km/s}^2$

Fig. 1 RMS position error against time with different process noises

For the PF-based filters, we set the drawn particles size as $N = 300$ to balance the execute time and the estimate accuracy. As indicated in [27], the refinement policy

of samples provides little improvement for the parameter performance. All the simulated calculations converge successfully, and the track loss rates are zero for all the filters discussed in this subsection.

3.1.1 Effect of the process noise

Here, we will study and analyze the filtering performance of the algorithms in comparison by verifying the process noise, while the measurement noise is relatively small, i.e., higher signal-to-noise ratio. For this, the measurement noise standard deviation (STD) is fixed to 1.5 mrad and the three sets of the process noise STD are given as 0.005 km/s², 0.01 km/s² and 0.04 km/s², respectively. Fig. 1(b)–Fig. 1(d) show the RMS position error curves versus time. Tables 1–3 summarize the statistics including the mean and variance of the RMSE and values of the RTAMSE.

Table 1 Performance comparison ($\sigma_v = 0.005 \text{ km/s}^2$)

Algorithm	RMSE		RTAMSE/km
	Mean/km	Variance/km ²	
EKF	0.159	0.016	0.489
UKF	0.611	0.377	2.200
PF-EKF	0.331	0.138	0.451
PF-UKF	0.187	0.023	0.647
ATPF	0.104	0.006	0.789
CAPF	0.033	0.008	0.168

Table 2 Performance comparison ($\sigma_v = 0.01 \text{ km/s}^2$)

Algorithm	RMSE		RTAMSE/km
	Mean/km	Variance/km ²	
EKF	0.103	0.004	0.365
UKF	0.241	0.073	0.575
PF-EKF	0.254	0.066	0.389
PF-UKF	0.137	0.016	0.437
ATPF	0.079	0.002	0.490
CAPF	0.031	0.001	0.167

Table 3 Performance comparison ($\sigma_v = 0.04 \text{ km/s}^2$)

Algorithm	RMSE		RTAMSE/km
	Mean/km	Variance/km ²	
EKF	0.081	0.004	0.413
UKF	0.081	0.007	0.385
PF-EKF	0.111	0.007	0.449
PF-UKF	0.090	0.001	0.443
ATPF	0.100	0.005	0.707
CAPF	0.048	0.001	0.168

Both qualitative results in Fig. 1(b) and quantitative statistics in Table 1 demonstrate that the measurement noise is relatively large when the process noise is 0.005 km/s², the RMS position error curve of the UKF shows the largest overall deviation trajectory difference, and the tracking performance is the worst one among the filters in comparison. The PF-EKF and PF-UKF show a larger bias than the EKF obviously in the smooth CV motion phase. This is

mainly because that the first-order Taylor series linearization error is relatively small when the process noise is mild enough. The RMS position errors of the ATPF and the CAPF are significantly smaller, mainly because of the usage of current observation and the target kinetics features as auxiliary variables during the locating procedure. The filters can capture the abruptly target maneuvering motion more accurately in real time. With respect to the RTAMSE parameter, after the end of maneuvering motion, the CAPF shows a significantly more accurate estimate than the ATPF, mainly owing to the usage of measurement constraints.

Simulation results exhibit that as the process noise increases, the tracking performance becomes worse during the smooth CV motion procedure and better in the maneuvering motion procedure. For all the three cases in discussion, the CAPF has the smallest RMSE and RTAMSE, and it implies a better estimate consistency, stronger robustness and better unbiasedness, respectively.

In addition, Table 4 summarizes the average execution time required for 100 Monte Carlo runs in the second case. Evidently, the PF-based methods show a higher calculation burden mainly due to the additional sampling computation. Compared with the PF-EKF and PF-UKF, the ATPF and CAPF show advantages in terms of the implementation in real time. The CAPF does not cost much more time than that of the ATPF for the additional optimization.

Table 4 Comparison of the execution time for 100 Monte Carlo runs

Algorithm	EKF	UKF	EPF	UPF	ATPF	CAPF
Time/s	3.03	17.81	78.24	64.83	17.68	19.49

3.1.2 Effect of the measurement noise

To study the effect of the measurement noise, we fix the process noise STD as 0.01 km/s² and set three sets of measurement noise STD as 0.5 mrad, 1.5 mrad and 3 mrad, respectively. Note that the second case here is the same as the second case in Section 3.1.1, and it is not repeatedly reported. Fig. 2(a), Fig. 1(c) and Fig. 2(b) report the resulting RMS position error curves versus time. Tables 5, 2, and 6 summarize the statistics of the RMSE and RTAMSE.

Table 5 Performance comparison ($\sigma_e = 0.5 \text{ mrad}$)

Algorithm	RMSE		RTAMSE/km
	Mean/km	Variance/km ²	
EKF	0.039	0.001	0.143
UKF	0.052	0.002	0.146
PF-EKF	0.068	0.006	0.152
PF-UKF	0.034	0.000 5	0.140
ATPF	0.030	0.000 4	0.202
CAPF	0.032	0.000 8	0.198

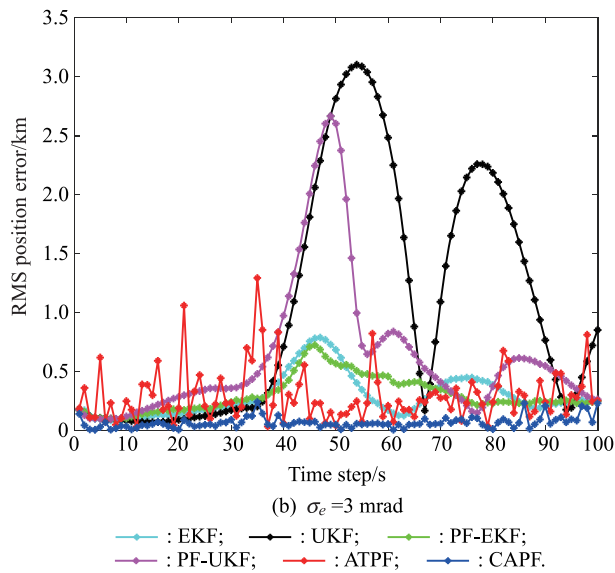
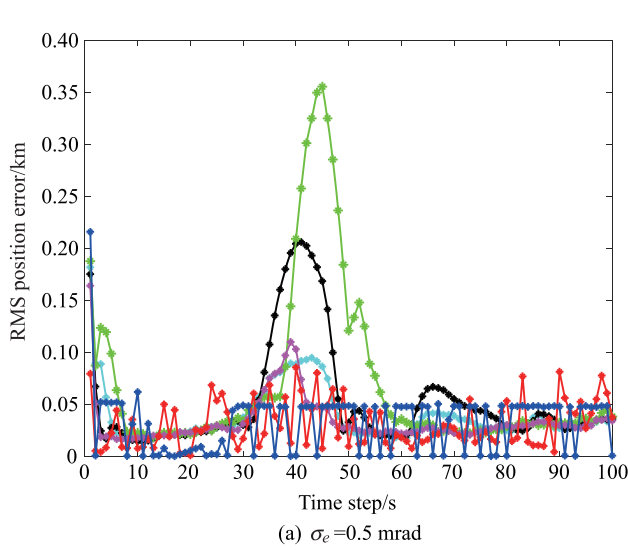


Fig. 2 RMS position error versus time under different measurement noises

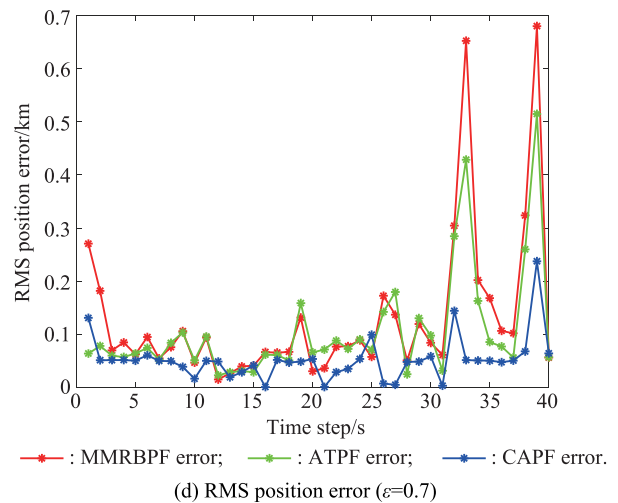
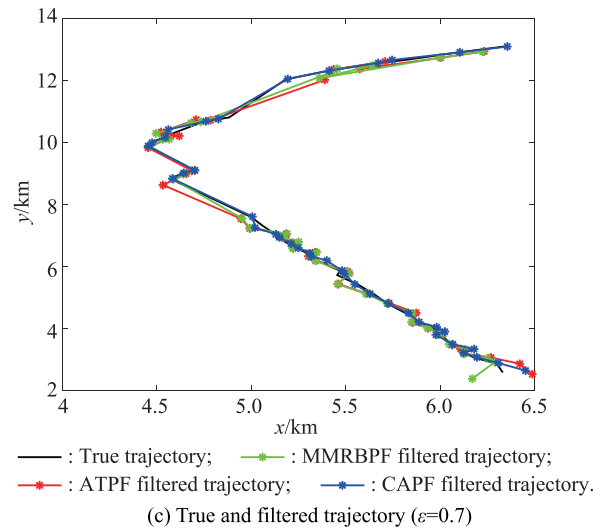
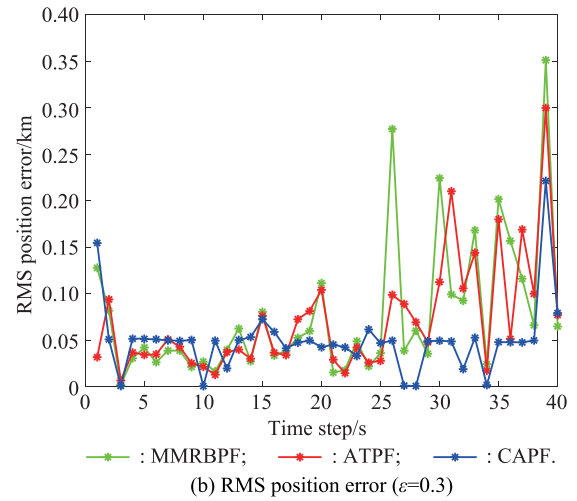
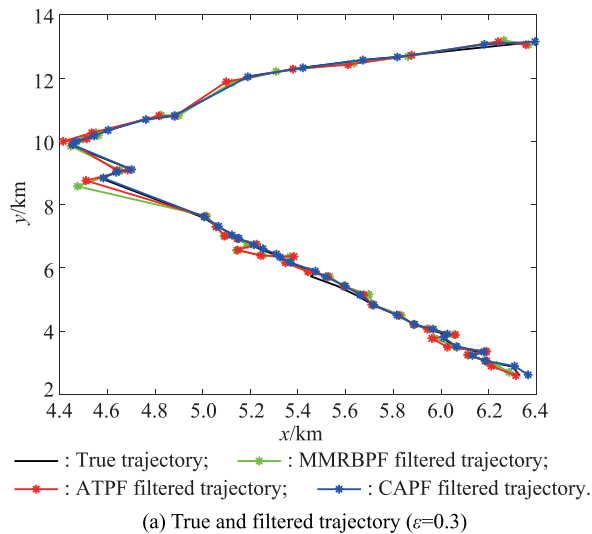


Fig. 3 Performance of MMRBPF, ATPF and CAPF

Simulation results exhibit that with the increment of observation noise, both the RMSE and RTAMSE show an increment for all the algorithms in comparison. The CAPF

has the smallest errors, demonstrating the superiority in terms of accuracy and robustness.

Table 6 Performance comparison ($\sigma_e = 3$ mrad)

Algorithm	RMSE		RTAMSE/km
	Mean/km	Variance/km ²	
EKF	0.189	0.086	0.667
UKF	0.616	0.371	2.021
PF-EKF	0.210	0.011	0.698
PF-UKF	0.331	0.102	1.035
ATPF	0.205	0.022	1.317
CAPF	0.051	0.001	0.281

3.2 Aperiodic and sparse sampling case

Now, we will discuss the bearings-only target maneuvering tracking in the aperiodic and sparse sampling scenario.

3.2.1 Gaussian mixed model noise

We will analyze a thorough and realistic performance comparison for the non-Gaussian noise mode in this subsection. The associated measurement noise probability density, $p(e_k)$, can be computed as

$$p(e_k) = (1 - \varepsilon)N(w; \mu_1; \mathbf{R}_1) + \varepsilon N(w; \mu_2; \mathbf{R}_2) \quad (35)$$

where e_k is the measurement noise independent of the state distribution; the parameter $\varepsilon \in [0, 1]$ is the weighting factor for the two components.

The STD of the two independently distributed Gaussian noise is set as

$$\begin{aligned} \mathbf{R}_1 &= \begin{bmatrix} (1 \text{ mrad})^2 & 0 \\ 0 & (1 \text{ mrad})^2 \end{bmatrix} \\ \mathbf{R}_2 &= \begin{bmatrix} (5 \text{ mrad})^2 & 0 \\ 0 & (5 \text{ mrad})^2 \end{bmatrix}. \end{aligned} \quad (36)$$

The first two moments of Gaussian mixed model (GMM) noise are

$$\mu = E(e) = (1 - \varepsilon)\mu_1 + \varepsilon\mu_2 \quad (37)$$

$$\begin{aligned} P(e) &= E((e - \mu)(e - \mu)^T) = \\ &= (1 - \varepsilon)P_1 + \varepsilon P_2 + \tilde{P} \end{aligned} \quad (38)$$

where

$$\tilde{P} = (1 - \varepsilon)\mu_1\mu_1^T + \varepsilon\mu_2\mu_2^T - \mu\mu^T. \quad (39)$$

For the simulations in this section, ε is set to 0.3 and 0.7 to simulate the glint noise which always has a thicker tail. The STD of the process noise is set to 0.01 km/s².

When $\varepsilon = 0.3$, the interacting multiple model EKF (IMMEKF) diverges when the object is missed from the observation at $t = 25$ s due to the stochastic larger sampling

interval, and the tracking loss rate is as high as 40%. During the maneuvering target tracking period $t = 25$ s to $t = 33$ s, the interacting multiple model UKF (IMMUKF) has a bias peak larger than 2.5 km. When $\varepsilon = 0.7$, the IMMEKF diverges, and the tracking loss rate is 100%. The IMMUKF shows a tracking divergence at $t = 25$ s, the track loss rate is as high as 40%. The major reason is the limitation of the Gaussian model, i.e., the likelihood should be unimodal. However, these requirements cannot be satisfied for the case of sparse sampling and the mixed Gaussian noise. Furthermore, the conventional EKF and UKF cannot work well to produce the importance distribution due to the major limitation of the Gaussian model [26]. Thus, we compare the MMRBPF, ATPF and the proposed CAPF for the GMM scenario in this section. The particles number is set to 100, and 100 Monte Carlo simulations are carried out independently.

Fig. 3(a) and Fig. 3(c) show the true and filtered trajectories for the two cases, respectively. Fig. 3(b) and Fig. 3(d) exhibit the RMS position errors of the MMRBPF, ATPF and CAPF for the two scaling factors respectively. All the filters could track the maneuvering target with zero loss rate. The proposed CAPF shows the superiority in terms of accuracy and robustness.

For $\varepsilon = 0.7$, the estimate bias of MMRBPF and ATPF become larger obviously, which is mainly because that the influence of glint noise is enhanced. Meanwhile, the CAPF presents the consistent robustness, mainly because that the adaptive particles sampled from the modified optimal proposal distribution could characterize the posterior PDF well. Hence, the CAPF can handle the nonlinear, non-Gaussian and online sparse sampling cases for the bearings-only maneuvering target tracking.

3.2.2 Effect of the sample size

To study the effect of the sample size onto the filtering performance, we chose four sets as 40, 100, 200 and 300, the other parameters are set as the same as the second case in Section 3.2.1.

Fig. 4 reports the RMS position error curves and the calculation time required for 100 Monte Carlo simulations with the variant particle sizes. Results reveal that the filtering performance of MMRBPF, ATPF and CAPF tend to be stable since the number of particles is 100. After that, the estimate error cannot be reduced significantly yet the computation time is still increased. Since the resampling step in the second stage is omitted, the calculation load of the CAPF is much less than that of MMRBPF, and a little more than that of the ATPF due to the optimization.

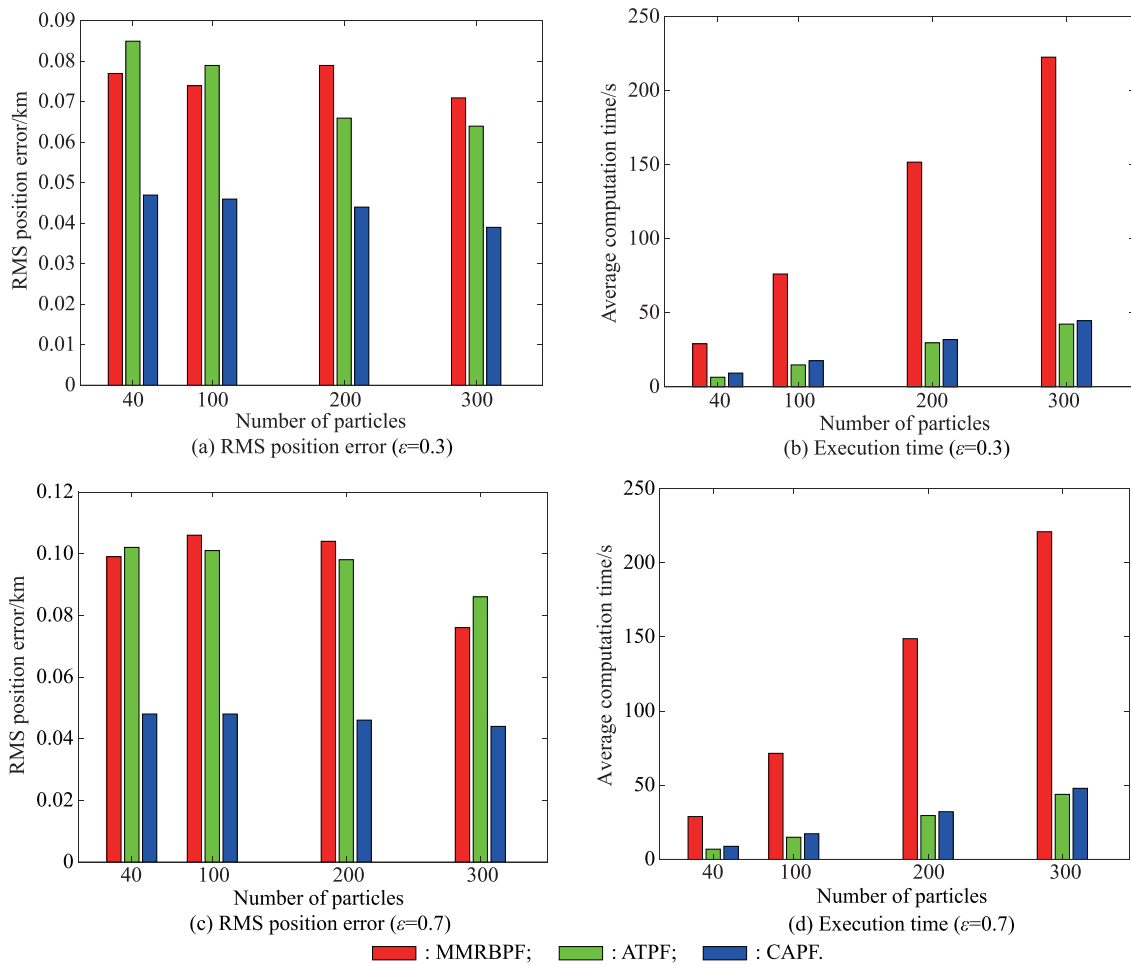


Fig. 4 Performance of MMRBPF, ATPF and CAPF with different particle numbers

4. Conclusions

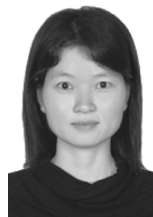
The paper presents the CAPF to track the nonlinear non-Gaussian bearings-only maneuvering target accurately on-line. The soft measurement constraint is implemented into the APF routine via adding the ℓ_1 regulation. Through doing this, the samples can be restricted into the feasible area. Meanwhile, the target kinetics features are incorporated into the update routine as the auxiliary variables, yielding significant samples efficiently. Furthermore, the proposal distribution is constructed as the Gaussian mixture, allowing the adaption and feedback from the original and the past observations simultaneously. The effect is weighted by the fuzzy factors, respectively. Additionally, since the CAPF only consists of one resampling step in the first stage each time, both the potential additional outlier error and the computation complexity are reduced notably. The model structural refinement is not necessary. Future work consists of the combination of the multiple motion modeling and the extension of the data association to track multiple maneuvering target scenes in clutter environment.

References

- [1] NARDONE S C, LINDGREN A G, KAI F G. Fundamental properties and performance of conventional bearings-only target motion analysis. *IEEE Trans. on Automatic Control*, 1984, 29(9): 775–787.
- [2] BAR-SHALOM Y, LI X R, KIRUBARAJAN T. Estimation with applications to tracking and navigation. Hoboken, NJ: Wiley, 2001.
- [3] SONG T L. Observability of target tracking with range-only measurements. *IEEE Trans. on Aerospace and Electronic Systems*, 1996, 32(4): 1468–1472.
- [4] YE M, ANDERSON B D O, YU C. Bearing-only measurement self-localization, velocity consensus and formation control. *IEEE Trans. on Aerospace and Electronic Systems*, 2017, 53(2): 575–586.
- [5] LI X R, JILKOV V P. A survey of maneuvering target tracking: approximation techniques for nonlinear filtering. *Signal and Data Processing of Small Targets*, 2004, 5428(62): 537–550.
- [6] JULIER S J, UHLMANN J K. Unscented filtering and nonlinear estimation. *Proceedings of the IEEE*, 2004, 92(3): 401–422.
- [7] LI W, CONG M, JIA Y, et al. Recursive filtering for complex networks using non-linearly coupled UKF. *IET Control Theory & Applications*, 2018, 12(4): 549–555.
- [8] ANDIEU C, DOUCET A, HOLENSTEIN R. Particle Markov

- Chain Monte carlo methods. *Journal of the Royal Statistical Society*, 2010, 72(3): 269–342.
- [9] BERTORP K, GROVER P. Feedback particle filter with data-driven gain-function approximation. *IEEE Trans. on Aerospace and Electronic Systems*, 2018, 54(5): 2118–2130.
 - [10] MERWE R V D, DOUCET A, FREITAS N D, et al. The unscented particle filter. *Proc. of the International Conference on Neural Information Processing Systems*, 2000: 563–569.
 - [11] KONATOWSKI S, KANIEWSKI P, MATUSZEWSKI J. Comparison of estimation accuracy of EKF, UKF and PF filters. *Annual of Navigation*, 2016, 23(1): 69–87.
 - [12] PITT M K, SHEPHARD N. Filtering via simulation: auxiliary particle filters. *Publications of the American Statistical Association*, 1999, 94(446): 590–599.
 - [13] ÚBEDA-MEDINA L, ÁNGEL F, GARCÍA-FERNÁNDEZ, GRAJAL J. Adaptive auxiliary particle filter for track-before-detect with multiple targets. *IEEE Trans. on Aerospace and Electronic Systems*, 2017, 53(5): 2317–2330.
 - [14] LI X R, JILKOV V P. Survey of maneuvering target tracking. Part V. Multiple-model methods. *IEEE Trans. on Aerospace and Electronic Systems*, 2005, 41(4): 1255–1321.
 - [15] HENK A P, BAR-SHALOM, YAAKOV BLOM. The interacting multiple model algorithm for systems with markovian switching coefficients. *IEEE Trans. on Automatic Control*, 1988, 33(8): 780–783.
 - [16] LI J, ZHOU D, QIN L. Tracking filter for nonballistic near space targets based on MVSIMM algorithm. *Proc. of the IEEE International Conference on Information and Automation*, 2015: 1899–1904.
 - [17] GARCÍA-FERNÁNDEZ Á F, SVENSSON L, MORELANDE M R, et al. Posterior linearization filter: principles and implementation using sigma points. *IEEE Trans. on Signal Processing*, 2015, 63(20): 5561–5573.
 - [18] GARCÍA-FERNÁNDEZ Á F, SVENSSON L, SÄRKKÄ S. Iterated posterior linearization smoother. *IEEE Trans. on Automatic Control*, 2017, 62(4): 2056–2063.
 - [19] SIMON D. Kalman filtering with state constraints: a survey of linear and nonlinear algorithms. *IET Control Theory & Applications*, 2010, 4(8): 1303–1318.
 - [20] LI X R. Compatibility and modeling of constrained dynamic systems. *Proc. of the International Conference on Information Fusion*, 2016: 240–247.
 - [21] GARCÍA-FERNÁNDEZ Á F, MORELANDE M R, GRAJAL J. Mixture truncated unscented Kalman filtering. *Proc. of the International Conference on Information Fusion*, 2012: 479–486.
 - [22] ZHANG Y G, CHENG R, HUANG Y L, et al. Truncated adaptive cubature particle filter. *Systems Engineering and Electronics*, 2016, 22(2): 383–391. (in Chinese)
 - [23] WANG J H, CAO J, LI W. Cost reference particle filter algorithm of intelligent optimization. *Systems Engineering and Electronics*, 2017, 39(12): 2857–2862. (in Chinese)
 - [24] PRÜFERT U, TRÖLTZSCH F, WEISER M. The convergence of an interior point method for an elliptic control problem with mixed control-state constraints. *Computational Optimization & Applications*, 2008, 39(2): 183–218.
 - [25] PRAKASH J, PATWARDHAN S C, SHAH S L. On the choice of importance distributions for unconstrained and constrained state estimation using particle filter. *Journal of Process Control*, 2001, 21(1): 3–16.
 - [26] AMOR N, BOUAYNAYA N, SHTERENBERG R, et al. On the convergence of constrained particle filters. *IEEE Signal Processing Letters*, 2017, 24(6): 858–862.
 - [27] ELVIRA V, MIGUEZ J, DJURIC P M. Adapting the number of particles in sequential Monte Carlo methods through an on-line scheme for convergence assessment. *IEEE Trans. on Signal Processing*, 2017, 65(7): 1781–1794.
 - [28] LI B, LIU C, CHEN W H. An auxiliary particle filtering algorithm with inequality constraints. *IEEE Trans. on Automatic Control*, 2017, 62(9): 4639–4646.
 - [29] KIM J, SUH T, RYU J. Inequality constrained Kalman filter for bearing-only target motion analysis. *Proc. of the International Conference on Control*, 2015: 1601–1607.
 - [30] LI L Q, XIE W X, LIU Z X. Auxiliary truncated particle filtering with least-square method for bearings-only maneuvering target tracking. *IEEE Trans. on Aerospace and Electronic Systems*, 2017, 52(5): 2562–2567.
 - [31] LINDSTEN F, BUNCH P, SÄRKKÄ, S, et al. Rao-Blackwellized particle smoothers for conditionally linear gaussian models. *IEEE Journal of Selected Topics in Signal Processing*, 2016, 10(2): 353–365.
 - [32] HOSTETTLER R, SARKKA S. Rao-Blackwellized Gaussian smoothing. *IEEE Trans. on Automatic Control*, 2018, 64(1): 305–312.
 - [33] ZHANG H, LI L, XIE W. Constrained multiple model particle filtering for bearings-only maneuvering target tracking. *IEEE Access*, 2018, 6: 51721–51734.
 - [34] KIM S J, KOH K, LUSTIG M, et al. An interior-point method for large-scale l_1 -regularized logistic regression. *IEEE Journal of Selected Topics in Signal Processing*, 2008, 1(4): 606–617.
 - [35] OZGEN S, ROSENTHAL F, MAYER J, et al. Retraction of data association probabilities via convex optimization. *Proc. of the 21st International Conference on Information Fusion*, 2018: 2430–2436.

Biographies



ZHANG Hongwei was born in 1982. She is currently pursuing her Ph.D. degree in the College of Information Engineering at Shenzhen University. She received her B.S. degree in electronic engineering from Zhengzhou University in 2006 and M.S. degree from South China University of Technology in 2013. Her research interests are particle filtering and multiple target tracking.
E-mail: hongweiz@szu.edu.cn



XIE Weixin was born in 1941. He received his B.S. degree from Xidian University, Xi'an, and joined the faculty of Xidian University in 1965. From 1981 to 1983, he was a visiting scholar with the University of Pennsylvania, USA. In 1989, he was invited to University of Pennsylvania as a visiting professor. He is currently a professor with Shenzhen University. His research interests include intelligent information processing and pattern recognition.
E-mail: wxxie@szu.edu.cn